

Engineering Notes

ENGINEERING NOTES are short manuscripts describing new developments or important results of a preliminary nature. These Notes should not exceed 2500 words (where a figure or table counts as 200 words). Following informal review by the Editors, they may be published within a few months of the date of receipt. Style requirements are the same as for regular contributions (see inside back cover).

Equilibrium-to-Equilibrium Maneuvers of Rigid Electrodynamic Tethers

Kalyan K. Mankala* and Sunil K. Agrawal†
University of Delaware, Newark, Delaware 19716

I. Introduction

SATELLITE tether systems have received much attention over the past two decades, for their cost-effective nature, in numerous space applications. Missions such as capture of nonfunctional satellites to put them into graveyard orbits^{1,2} and transfer of satellites from low Earth orbits (LEOs) to geostationary Earth orbits³ have been conceptually designed with tether systems. These missions involve the rendezvous of the tether end with a target. Guidance and control strategies are required to manipulate the tether end to allow this critical step of rendezvous to happen. Also, applications such as deorbiting or reboosting can benefit by maintaining tether at an angle to maximize the electromagnetic force. Gravity gradient tends to stabilize a nonconducting tether to a radial configuration, whereas electrodynamic forces present in a conducting tether sway the tether away from the radial configuration. Forward et al.⁴ discuss the optimization of the tether angle at which the component of electrodynamic force in the tangential direction can be maximized while having a stable tether configuration. They also mention briefly the idea of using a control resistor for the control of tether angle. This is the motivation behind the work presented in this Note. We consider the problem of maneuver of tether from one equilibrium configuration to another to show the effectiveness of a control resistor.

In the literature, electrodynamic tethers are modeled mainly as massless rigid bodies with some tip mass⁵ or as a rigid tether with distributed mass.⁶ In this Note, we model the tether as a rigid body with distributed mass. The gravity gradient that exists along the length of the tether is modeled while considering the dynamics of the tether. Because the magnetic field varies as $1/r^3$, we assume a constant magnetic field along the length of the tether. It is observed that both linear and nonlinear current-voltage (I-V) characteristics are used in the literature when the electrodynamic tether problem is examined. Forward et al.⁴ and Corsi and Iess⁷ use the linear I-V characteristics to discuss the deorbiting issues in an electrodynamic tether. Pelaez et al.⁶ and Dobrowolny⁸ use a nonlinear I-V model to study the dynamic instabilities in an electrodynamic tether. Because the main aim of this Note is to study the use of a control resistor

as an actuator, we have used a linear I-V model to emphasize the control problem. This will also provide an insight into using the control resistor for nonlinear I-V characteristics case.

The primary contribution of this Note is that we use a variable resistor in series with the tether as the control parameter for equilibrium to equilibrium maneuvers. The tether angle can also be modified by applying a torque input at the joint. However, this is unrealistic when working with a tether system. The use of a variable resistor helps in achieving various stable equilibrium solutions in the $[-\pi, 0]$ range, as opposed to the existence of only two stable equilibrium solutions when a fixed resistor is used with torque control input. This point will be discussed in more detail in the following sections. Also, we believe that the method of changing the resistance of the circuit is more energy efficient than applying a torque. Moreover, when the tether is modeled as a variable length flexible body, a boundary control, in the form of drum torque input, leaves the system highly underactuated. In these situations, a variable resistor can be used along with the torque input to improve the controllability of the system. Our contributions are summarized as follows: 1) The tether is modeled as a rigid body with distributed mass rather than as massless rigid body with tip mass as in existing models. Such a model allows a clear analytical description of relative equilibria on equatorial circular orbits. In the literature, there are no such analytical descriptions. 2) This in turn gave a direct insight into choosing a resistor in series with the tether as a control parameter. Control laws were developed in terms of this resistance for equilibrium to equilibrium maneuvers. Because the resistor can only increase the resistance from a nominal value, the change in resistance is only allowed to be positive from the nominal value. The positivity of the control resistance is assured through a strategic choice of gains. To the best of the authors' knowledge no control laws are studied in the literature for the manipulation of the tether angle; this is a new contribution of this Note.

The rest of the Note is organized as follows: In Sec. II, we look at the dynamics of a tether in magnetic equatorial orbits. In Sec. III, we discuss the possible equilibrium configurations of the tether when the satellite is restricted to circular orbits. In Sec. IV, we present feedback control laws to perform equilibrium to equilibrium maneuvers.

II. Dynamics of Tether

We consider a satellite of mass m_1 rotating around the Earth in the magnetic equatorial plane. A tether of length L and mass m_2 is attached to the satellite via a pin joint, about which it can freely rotate. The tether is modeled as a rigid body with mass m_c distributed along the length of the tether. Generally, the lengths of the tether are in the range of 5–50 km. Thus, a gravity gradient exists along the length of the tether. Because the magnetic field varies as $1/r^3$, we assume that it remains constant along the length of the tether. Forward et al.⁴ point out that aluminum is a good material for the tether because of its low resistivity ($27.4 \text{ n}\Omega \cdot \text{m}$), low density (2700 kg/m^3), and low cost compared to copper and silver. Therefore, we use an aluminum tether in our simulation studies. In the following section, we will develop the dynamics of the tether assuming that $L/r \ll 1$.

Let $X-Y$ be the inertial frame fixed to the center of the Earth. The configuration of the system at some time t can be described by the parameters r , θ_1 , and θ_2 (Fig. 1), where r is the radial position of the satellite from the center of the Earth, θ_1 is the angular position of the satellite measured from X , and θ_2 is the angle of the tether in the orbital frame ($\hat{e}_r - \hat{e}_\theta$). Here $\hat{b}_1 - \hat{b}_2$ represents the tether

Received 8 December 2003; revision received 15 November 2004; accepted for publication 18 November 2004. Copyright © 2004 by the American Institute of Aeronautics and Astronautics, Inc. All rights reserved. Copies of this paper may be made for personal or internal use, on condition that the copier pay the \$10.00 per-copy fee to the Copyright Clearance Center, Inc., 222 Rosewood Drive, Danvers, MA 01923; include the code 0731-5090/05 \$10.00 in correspondence with the CCC.

*Graduate Student, Department of Mechanical Engineering; mankala@me.udel.edu. Student Member AIAA.

†Professor, Department of Mechanical Engineering; agrawal@me.udel.edu.

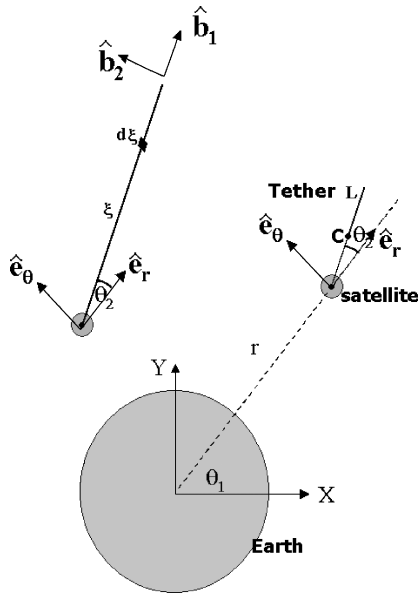


Fig. 1 Satellite tether model.

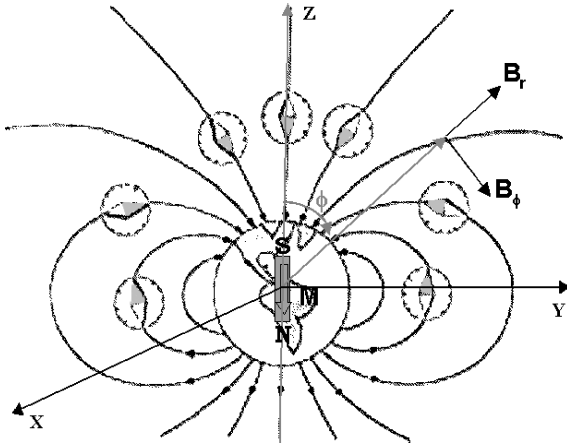


Fig. 2 Nontilted dipole model of Earth magnetic field.

attached local frame. Let l_c be the distance from the c.m. of the tether to satellite. In the following derivations, we assume that the tether mass is uniformly distributed, and so $l_c = L/2$. If the mass is not uniformly distributed or if there is a point mass (subsattellite) at the other end of the tether, then l_c needs to be suitably modified, but essentially the concept remains the same.

Let R_1 and R_2 be the thruster forces acting on the satellite that constrain it to rotate in a certain orbit that is essential to realize equilibrium configurations for the tether. Similar analysis given in the Note can be applied to an alternate formulation in which the center of mass of the whole system is assumed to have the prescribed motion instead of the satellite. In either case, because r and θ_1 have prescribed motion, we derive only θ_2 dynamics in this section. Let F be the electrodynamic force acting on the tether. Given a model of the Earth's magnetic field, we can derive this force using the basic laws of electromagnetics.⁹ In this Note, we consider a nontilted, Earth-centered dipole model for the magnetic field of the Earth^{6,10,11} (Fig. 2). The dipole strength M_{dp} is taken as $7.78810^{22} \text{ A} \cdot \text{m}^2$ (obtained from International Geomagnetic Reference Field 2000 values). Using this dipole model, we can express the magnetic field in the equatorial plane as $\mathbf{B} = (\mu_0 M / 4\pi r^3) \hat{\mathbf{k}}$.

A. Electrodynamic Force

The velocity of an element $d\xi$ of the tether at a distance ξ from the satellite is

$$\mathbf{V}_{d\xi} = \dot{r} \hat{\mathbf{e}}_r + r \dot{\theta}_1 \hat{\mathbf{e}}_\theta + \xi (\dot{\theta}_1 + \dot{\theta}_2) \hat{\mathbf{b}}_2 \quad (1)$$

Using Faraday's law of induction, we can find the induced emf ε in the tether due to the motion of the tether in the magnetic field of the Earth as

$$\begin{aligned} \varepsilon &= \int d\varepsilon = \int_0^L \mathbf{V}_{d\xi} \times \mathbf{B} \hat{\mathbf{k}} \cdot d\xi \hat{\mathbf{b}}_1 \\ &= BL \left[-\dot{r} \sin(\theta_2) + r \dot{\theta}_1 \cos(\theta_2) + \frac{L}{2} (\dot{\theta}_1 + \dot{\theta}_2) \right] \end{aligned} \quad (2)$$

When linear current-voltage characteristics are assumed, that is, $I = \varepsilon / \text{Res}$, where Res is the resistance of the tether, the electrodynamic force experienced by the current carrying tether in the magnetic field can be calculated as

$$\begin{aligned} \mathbf{F} &= \int d\mathbf{F} = \int_0^L I (d\xi \hat{\mathbf{b}}_1 \times \mathbf{B} \hat{\mathbf{k}}) \\ &= - \underbrace{\frac{B^2 L^2}{\text{Res}} \left[-\dot{r} \sin(\theta_2) + r \dot{\theta}_1 \cos(\theta_2) + \frac{L}{2} (\dot{\theta}_1 + \dot{\theta}_2) \right]}_F \hat{\mathbf{b}}_2 \end{aligned} \quad (3)$$

Forward et al.⁴ derive a similar expression for electrodynamic force on a rigid tether in circular orbit ($\dot{r} = 0$) at a constant tilt from the local vertical ($\theta_2 = 0$).

B. Equations of Motion

Dynamics of the motion of θ_2 can be obtained from the Lagrange's equation as follows:

$$\frac{\partial}{\partial t} \frac{\partial L}{\partial \dot{\theta}_2} - \frac{\partial L}{\partial \theta_2} = F_{\theta_2} \quad (4)$$

where $L = K - V$ and K is kinetic energy and V is potential energy. The generalized force F_{θ_2} in Eq. (4) can be derived considering the virtual work done by the external forces acting on the system,

$$\begin{aligned} \delta W &= F_{\theta_2} \delta \theta_2 = \int_0^L -\frac{F}{L} d\xi \hat{\mathbf{b}}_2 \times \xi \hat{\mathbf{b}}_1 \cdot \delta \theta_2 \hat{\mathbf{k}} \\ \Rightarrow F_{\theta_2} &= -\frac{FL}{2} \end{aligned} \quad (5)$$

The kinetic energy K and potential energy V of the system can be written as

$$\begin{aligned} K &= \frac{1}{2} m_1 (\dot{r}^2 + r^2 \dot{\theta}_1^2) + \frac{1}{2} m_c \left\{ [\dot{r} - l_c (\dot{\theta}_1 + \dot{\theta}_2) \sin(\theta_2)]^2 \right. \\ &\quad \left. + [r \dot{\theta}_1 + l_c (\dot{\theta}_1 + \dot{\theta}_2) \cos(\theta_2)]^2 \right\} + \frac{1}{2} I_c (\dot{\theta}_1 + \dot{\theta}_2)^2 \end{aligned} \quad (6)$$

$$V = - \underbrace{\frac{GMm_1}{r}}_{V_1} - \underbrace{\frac{GMm_c}{L} \int_0^L \frac{1}{\sqrt{r^2 + \xi^2 + 2r\xi \cos(\theta_2)}} d\xi}_{V_2} \quad (7)$$

To avoid singularities in V_2 , we expand it in Taylor series of L/r , neglecting terms of order $(L/r)^3$ and higher,

$$\begin{aligned} V_2 &= (-GMm_c) \left\{ 1 - [\cos(\theta_2)/2](L) \right. \\ &\quad \left. + \left[-\frac{1}{6} + \frac{1}{2} \cos^2(\theta_2) \right] (L)^2 \right\} \end{aligned} \quad (8)$$

Substituting the expressions for K , V and F_{θ_2} in Eq. (4), we get

$$\begin{aligned} \frac{m_c L^2}{3} \ddot{\theta}_2 &= m_c \frac{L}{2} \sin(\theta_2) (\ddot{r} - r \dot{\theta}_1^2) - m_c \frac{L}{2} \cos(\theta_2) (r \ddot{\theta}_1 + 2\dot{r} \dot{\theta}_1) \\ &\quad - \frac{m_c L^2}{3} \ddot{\theta}_1 + \frac{GMm_c \sin(\theta_2)}{r} \left[\frac{1}{2} \left(\frac{L}{r} \right) - \left(\frac{L}{r} \right)^2 \cos(\theta_2) \right] \\ &\quad - \frac{B^2 L^3}{2\text{Res}} \left[-\dot{r} \sin(\theta_2) + r \dot{\theta}_1 \cos(\theta_2) + \frac{L}{2} (\dot{\theta}_1 + \dot{\theta}_2) \right] \end{aligned} \quad (9)$$

III. Circular Orbit: Equilibrium Solutions

If the reference orbit followed by the satellite is a circular orbit ($\omega = \dot{\theta}_1 = \sqrt{GM/r^3}$), then $\dot{\theta}_1 = 0$, and $\ddot{r} = 0$, and $\dot{r} = 0$. We can simplify Eq. (9) as

$$(m_c L^2 / 3) \ddot{\theta}_2 = -m_c L^2 \dot{\theta}_1^2 \sin(\theta_2) \cos(\theta_2) - (B^2 L^3 / 2 \text{Res}) \times [r \dot{\theta}_1 \cos(\theta_2) + (L/2)(\dot{\theta}_1 + \dot{\theta}_2)] \quad (10)$$

Furthermore, if there is an equilibrium for θ_2 , then $\dot{\theta}_2 = 0$, and $\ddot{\theta}_2 = 0$. Substituting these in the preceding equation of motion, we get

$$-m_c L^2 \dot{\theta}_1^2 \sin(\theta_2) \cos(\theta_2) - (B^2 L^3 / 2 \text{Res}) [r \dot{\theta}_1 \cos(\theta_2) + (L/2) \dot{\theta}_1] = 0 \quad (11)$$

For a choice of system variables, the numerical solutions of θ_2 of Eq. (11) are closely related to the following approximate analytical expressions:

$$\begin{aligned} \cos(\theta_2) &\approx -\frac{L}{2r}, & \text{Res} < \frac{B^2 L r}{2m_c \dot{\theta}_1} \\ \cos(\theta_2) &\approx -\frac{L}{2r}, & \sin(\theta_2) &\approx -\frac{B^2 L r}{2m_c \dot{\theta}_1 \text{Res}}, & \text{Res} > \frac{B^2 L r}{2m_c \dot{\theta}_1} \end{aligned} \quad (12)$$

We know that the tether has some internal resistance because of its material properties. For example, an aluminum tether, of length $L = 5$ km and area of cross section $A = 3.14$ mm², will have an inherent resistance of $\text{Res}_i = 43.6$ Ω . We can view Res as a control resistor Res_u in series with the inherent tether resistance Res_i . We can change the control resistance Res_u to any desired positive value and, thus, change Res . From Eq. (12), it is clear that for different values of Res , we can get different equilibrium values, all lying in the $[0, -\pi]$ range. No matter what value of Res_u we choose, there are always two equilibrium values close to $-(\pi/2)$ and $+(\pi/2)$ (because $L/2r \ll 1$). All of the simulations and examples here are performed for a satellite rotating in a circular orbit of radius $r = 7671$ km, with an aluminum tether of length $L = 5$ km and area of cross section $A = \pi$ mm².

A. Point-to-Point Motion with Natural Damping

Because the electrodynamic force acts as drag force, the system will have certain stable equilibrium solutions. In fact all of the possible solutions in the $[-\pi, 0]$ range, discussed in this section, are stable equilibrium solutions for an appropriate value of resistance. For example, for a control resistance $\text{Res}_u = 545.8$ Ω , $\theta_2 = -165.93$ deg, and -14.08 deg are stable equilibrium solutions (Fig. 3). We know that every stable equilibrium solution has its own domain of attraction. Therefore, this idea can be used to move the system from one equilibrium to another. However, because the system is lightly damped, we expect that it might take a long time for the tether to come to equilibrium.

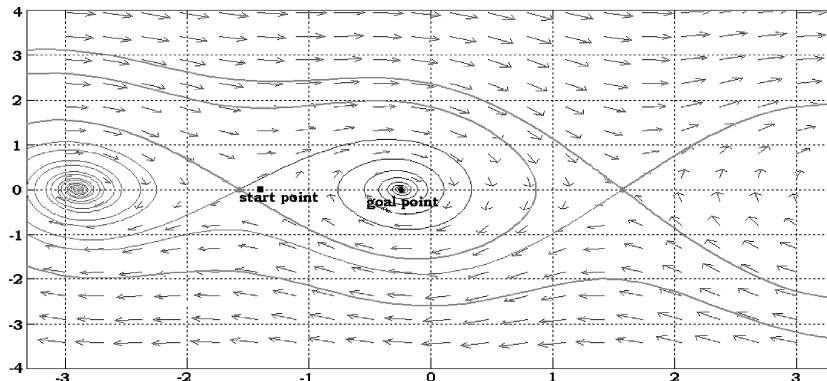


Fig. 3 Phase plot $\dot{\theta}_2$ Vs θ_2 when $\text{Res}_u = 545.8$ Ω .

B. Natural Damping: Example

If the tether is in equilibrium at $\theta_2 = -82.82$ deg, which corresponds to $\text{Res}_u = 101.2$ Ω , and we want it move to $\theta_2 = -14.08$ deg, which corresponds to $\text{Res}_u = 545.8$ Ω , then an instantaneous change of Res_u from 101.2 Ω to 545.8 Ω makes the initial point lie in the domain of attraction of the target point (Fig. 3). From Fig. 4, we can see that, with natural damping alone, the tether oscillates about the target point and takes more than 360 days to come to equilibrium at that point.

IV. Feedback Control Law: Set Point Control

In Sec. III, we see that the response of the system with natural damping alone is not desirable. In this section, we develop a feedback control law for the variable resistor to achieve faster equilibrium to equilibrium maneuvers. In the following discussion, θ_{20} represents the initial tether equilibrium angle and θ_{2f} the final tether equilibrium angle to be achieved. To achieve a feedback linearized system, we need to cancel the nonlinear terms in the dynamic equation of θ_2 . This is achieved by considering the following control law:

$$\begin{aligned} \text{Res}_u = & \frac{\overbrace{(3B^2 L / 2m_c) r \dot{\theta}_1 [\cos(\theta_2) + (L/2r)]}^{\text{term1}} + \overbrace{(3B^2 L^2 / 4m_c) \dot{\theta}_2}^{\text{term2}}}{\underbrace{K_1 \dot{\theta}_2}_{\text{term3}} + \underbrace{K_2 (\theta_2 - \theta_{2f}) - 3\dot{\theta}_1^2 \sin(\theta_2) \cos(\theta_2)}_{\text{term4}}} - \text{Res}_i \end{aligned} \quad (13)$$

The choice of the gains K_1 and K_2 should take into consideration the constraint that Res_u should always be positive. Note that term1/term4 is always positive when θ_2 lies in the $[0, -\pi]$ range (except in the vicinity of $-\pi/2$) in which all equilibrium configurations are located. In fact, term1/term4 $>$ Res_i at LEOs for typical tether properties (such as aluminum tether of 5-km length). Here term2 and term3 are transient terms; they die out with time. Therefore, if

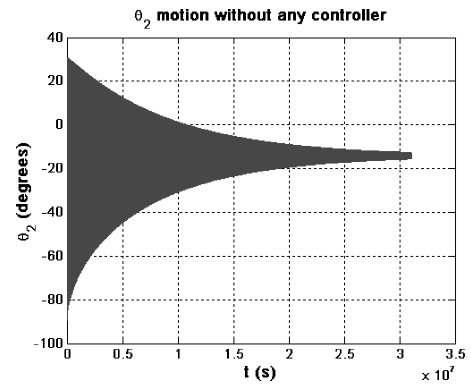


Fig. 4 Motion of tether from $\theta_2 = -82.82$ to $\theta_2 = -14.08$ deg with natural damping.

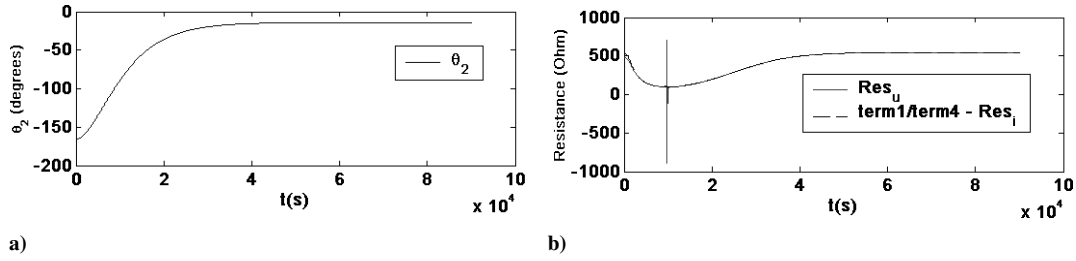


Fig. 5 Critically damped controller with $w_n = 1.7 \times 10^{-4}$, $\theta_{20} = -165.93$ deg and $\theta_{2f} = -14.08$ deg: a) $\theta_2(t)$ and b) $\text{Res}_u(t)$.

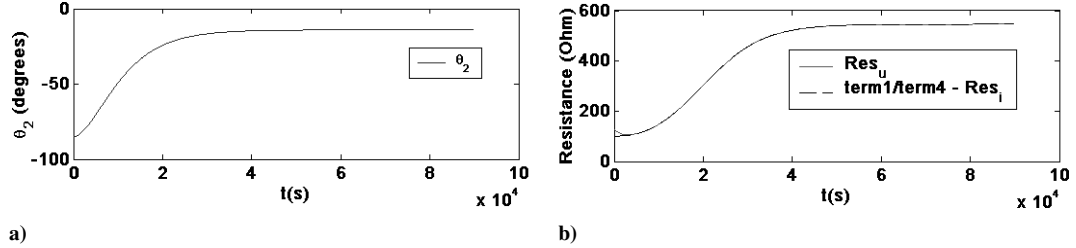


Fig. 6 Critically damped controller with $w_n = 1.7 \times 10^{-4}$, $\theta_{20} = -82.82$ deg and $\theta_{2f} = -14.08$ deg: a) $\theta_2(t)$ and b) $\text{Res}_u(t)$.

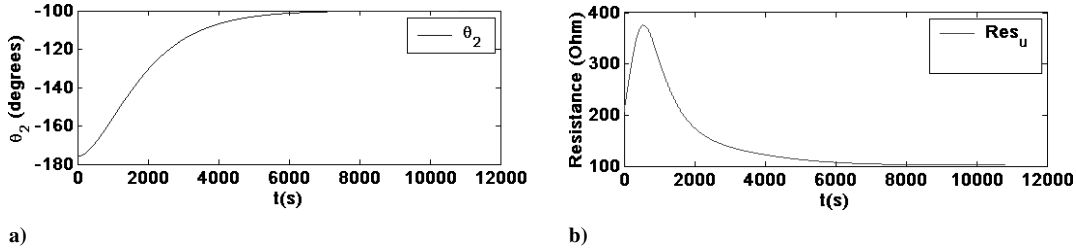


Fig. 7 Critically damped controller with $w_n = 0.001$, $\theta_{20} = -176$ deg and $\theta_{2f} = -100$ deg: a) $\theta_2(t)$ and b) $\text{Res}_u(t)$.

peak values of term2 and term3 are made an order of magnitude less than term1 and term4, respectively (by a proper choice of K_1 and K_2), then we can make sure that Res_u is always positive. Using the preceding control law to feedback linearize the system, we get the closed-loop dynamics as

$$\ddot{\theta}_2 = -K_1 \dot{\theta}_2 - K_2 (\theta_2 - \theta_{2f}) \quad (14)$$

Let $e = \theta_2 - \theta_{2f}$, $K_1 = 2\zeta w_n$, and $K_2 = w_n^2$; then, the closed-loop dynamics becomes

$$\ddot{e} + 2\zeta w_n \dot{e} + w_n^2 e = 0 \quad (15)$$

In Eq. (15), ζ and w_n have to be chosen such that the peak values of term2 and term3 are an order of magnitude less than term1 and term4, respectively. Toward this aim, we can consider three different type of controllers, 1) critically damped ($\zeta = 1$), 2) overdamped ($\zeta > 1$), and 3) underdamped ($\zeta < 1$). In the following paragraphs, we take a case of critically damped controller to find the control gains.

For this case, $K_1 = 2w_n$ and $K_2 = w_n^2$. Integrating the error dynamics gives $\theta_2(t)$, which can be differentiated to get $\dot{\theta}_2(t)$ and $\ddot{\theta}_2(t)$. Using the analytical solutions for $\theta_2(t)$, we have the following terms:

$$\begin{aligned} \text{term2: } (3B^2 L^2 / 4m_c) [-w_n^2 (\theta_{20} - \theta_{2f}) e^{-w_n t}] \\ \text{term3: } w_n^2 (\theta_{20} - \theta_{2f}) e^{-w_n t} (1 - w_n t) \end{aligned} \quad (16)$$

For a particular choice of system parameters $r = 7671$ km, $L = 5$ km, and $A = \pi \text{ mm}^2$, with tether material as aluminum, we have the following:

$$\begin{aligned} \text{term1: } \mathcal{O}(-4), \quad \text{term3: } w_n^2 \pi, \\ \text{term2: } \mathcal{O}(-4) (w_n^2 \pi / e), \quad \text{term4: } \mathcal{O}(-6) \end{aligned} \quad (17)$$

If $\text{term2} < \text{term1}/10$ and $\text{term3} < \text{term4}/10$, then $w_n \leq 1.7 \times 10^{-4}$.

Figure 5 shows the response of θ_2 for a step input, with a critically damped controller and $w_n = 1.7 \times 10^{-4}$. Note that $\text{Res}_u(t)$ is always positive and that the approximated curve $\text{term1}/\text{term4} - \text{Res}_i$ matches very closely the actual one. Figure 6 shows the response of $\theta_2(t)$ when $\theta_{20} = -82.82$ deg and $\theta_{2f} = -14.08$ deg. The tether comes to equilibrium at the final point within 25 h, which is small compared to 365 days using just natural damping (Sec. III.A).

Similarly gains can be chosen assuming underdamped and overdamped controllers. Note that there can be gains that do not necessarily make one term or the other an order of magnitude higher than the other. Because it is difficult to assure analytically the positivity of Res_u for such gains, a computer program can be used for this end. For example, $w_n = 0.001$ achieves the set point control in less time (3 h) but it does not fit the described category (Fig. 7).

V. Conclusions

The dynamics of an electrodynamic tether system is derived with the system restricted to an equatorial plane. The tether was modeled as a rigid body with mass distributed throughout the length. For the magnetic field of the Earth, we considered a nontilted, Earth-centered dipole model. Approximate analytical expressions for the relative equilibrium solutions of the tether are derived in terms of system parameters when the satellite is restricted to circular orbits. A variable resistor was chosen as a control parameter and feedback control laws were designed for equilibrium to equilibrium maneuvers. Gains of the feedback control laws were chosen with a strategy that can always achieve positivity of the control resistor because resistance can never be negative.

For a particular choice of system parameters, gains were found for critically damped controller such that the control resistance is always positive. Simulation results show the effectiveness of the feedback controller. The response time was considerably less for the feedback controller compared to the naturally damped system.

Simulation results with gains that cannot analytically assure the positivity of the control resistance but can achieve faster maneuvers are given.

Faster response times allow us to employ the control resistor effectively even when trajectories are not exactly circular and magnetic field varies over the orbit. This can be done by approximating the orbit as a combination of circular arcs and neglecting the small variations in the magnetic field over a circular arc. By employing control laws over different circular arcs, we can effectively control the tether angle.

During deorbiting or reboosting, it is practical to approximate the instantaneous orbit to a circular orbit. To optimize electrodynamic drag (or thrust) force in such cases, we can use the control resistor to control the librations of the tether and to maintain an optimum tether angle. In the real case, the tether cannot be treated as a rigid body. If it is modeled as a flexible body, then we have infinite degrees of freedom. In such a case, we can use a control resistor as an actuator, in addition to any boundary control, to improve the controllability of the system.

References

- ¹Mankala, K. K., and Agrawal, S. K., "Dynamic Modeling and Simulation of Satellite Tethered Systems," *Proceedings of the ASME Design Engineering Technical Conference*, Vol. 5A, American Society of Mechanical Engineers, 2003, pp. 379–388.
- ²Mankala, K. K., and Agrawal, S. K., "Dynamic Modeling and Simulation of Impact in Tether Net/Gripper Systems," *Multibody System Dynamics*, Vol. 11, No. 3, 2004, pp. 235–250.
- ³Lorenzini, E. C., Cosmo, M. L., Kaiser, M., Bangham, M. E., Vonderwell, D. J., and Johnson, L., "Mission Analysis of Spinning Systems for Transfers from Low Orbits to Geostationary," *Journal of Spacecraft and Rockets*, Vol. 37, No. 2, 2000, pp. 165–172.
- ⁴Forward, R. L., Hoyt, R. P., and Uphoff, C. W., "Terminator Tether: A Spacecraft Deorbit Device," *Journal of Spacecraft and Rockets*, Vol. 37, No. 2, 2000, pp. 187–196.
- ⁵Breakwell, J. V., Gearhart, J. W., "Eccentricity Perturbations on a Long Tumbling Dumbbell Satellite," *Advances in the Astronautical Sciences*, Vol. 75, Pt. 1, 1991, pp. 3–9.
- ⁶Pelaez, J., Lorenzini, E. C., Ruiz, M., and Lopez-Rebollal, O., "A New Kind of Dynamic Instability in Electrodynamic Tethers," *Journal of Astronautical Sciences*, Vol. 48, No. 4, 2000, pp. 449–476.
- ⁷Corsi, J., and Iess, L., "Stability Analysis and Control of Electrodynamic Tether for Deorbiting Applications," *Acta Astronautica*, Vol. 48, No. 5-12, 2001, pp. 491–501.
- ⁸Dobrowolny, M., "Lateral Oscillations of an Electrodynamic Tether," *Journal of Astronautical Sciences*, Vol. 50, No. 2, 2002, pp. 125–147.
- ⁹Resnick, R., and Halliday, D., "Faraday's Law of Induction," *Physics*, Wiley, New York, 1978.
- ¹⁰Vannaroni, G., Dobrowolny, M., and De Venuto, F., "Deorbiting with Electrodynamic Tethers: Comparison Between Different Tether Configurations," *Space Debris*, Vol. 1, No. 3, 1999, pp. 159–172.
- ¹¹Pelaez, J., and Lara, M., "Periodic Solutions in Electrodynamic Tethers on Inclined Orbits," *Journal of Guidance, Control, and Dynamics*, Vol. 26, No. 3, 2003, pp. 395–406.